JPET Fast Forward. Published on January 6, 2017 as DOI: 10.1124/jpet.116.238436
This article has not been copyedited and formatted. The final version may differ from this version.

Regulation of chemokine signal integration by Activator of G-protein Signaling 4 (AGS4)

William G. Robichaux, III, Melissa Branham-O'Connor, Il-Young Hwang, Ali Vural, John H. Kehrl and Joe B. Blumer

Department of Cell and Molecular Pharmacology and Experimental Therapeutics, Department of Neurosciences, Medical University of South Carolina, Charleston, SC 29425 (W.G.R., M.B.O., J.B.B.)

B-Cell Molecular Immunology Section, Laboratory of Immunoregulation, National Institute of Allergy and Infectious Diseases, National Institutes of Health, Bethesda, MD 20892 (I-Y.H., A.V., J.H.K.)

Downloaded from jpet.aspetjournals.org at ASPET Journals on April 24, 2024

JPET Fast Forward. Published on January 6, 2017 as DOI: 10.1124/jpet.116.238436
This article has not been copyedited and formatted. The final version may differ from this version.

Running Title: AGS4 in chemokine signal integration

Corresponding Author:

Joe B. Blumer

Department of Cell and Molecular Pharmacology and Experimental Therapeutics

Medical University of South Carolina

173 Ashley Ave, BSB358, MSC509

Charleston, SC 29425

Phone: (843) 792-3552

Email: blumerjb@musc.edu

Number of text pages: 32

Number of figures: 5

Number of references: 68

Number of words in the Abstract: 188

Number of words in the Introduction: 530

Number of words in the Discussion: 789

Abbreviations: Activator of G-protein Signaling (AGS), Regulator of G-protein Signaling (RGS), G-protein regulatory motif (GPR), G-protein signaling modulator (Gpsm), G-protein coupled receptor (GPCR), seven transmembrane receptor (7TMR), bioluminescence resonance energy transfer (BRET), pertussis toxin (PTX), complete blood count (CBC), extracellular signal-regulated kinase (ERK), dendritic cell (DC), N-formyl-methionine-leucine-phenylalanine (fMLP), intraperitoneal (IP), Guanine nucleotide-binding protein G(i), alpha subunit (Gnai)

Downloaded from jpet.aspetjournals.org at ASPET Journals on April 24, 2024

JPET Fast Forward. Published on January 6, 2017 as DOI: 10.1124/jpet.116.238436
This article has not been copyedited and formatted. The final version may differ from this version.

ABSTRACT

Activator of G-protein signaling 4 (AGS4)/G-protein signaling modulator 3 (Gpsm3) contains three G-protein regulatory (GPR) motifs, each of which can bind Gαi-GDP free of Gβγ. We previously demonstrated that the AGS4-Gαi interaction is regulated by seven transmembrane-spanning receptors (7-TMR), which may reflect direct coupling of the GPR-Gαi module to the receptor analogous to canonical Gαβγ heterotrimer. Here, we demonstrate that the AGS4-Gαi complex is regulated by chemokine receptors in an agonist-dependent manner that is receptor-proximal. As an initial approach to investigate the functional role(s) of this regulated interaction *in vivo*, we analyzed leukocytes, in which AGS4/Gpsm3 is predominantly expressed, from AGS4/Gpsm3-null mice. Loss of AGS4/Gpsm3 resulted in a mild but significant neutropenia and leukocytosis. Dendritic cells, T lymphocytes and neutrophils from AGS4/Gpsm3-null mice also exhibited significant defects in chemoattractant-directed chemotaxis and ERK activation. An *in vivo* peritonitis model revealed a dramatic reduction in the ability of AGS4/Gpsm3-null neutrophils to migrate to primary sites of inflammation. Taken together, these data suggest that AGS4/Gpsm3 is required for proper chemokine signal processing in leukocytes and provide further evidence for the importance of the GPR-Gαi module in the regulation of leukocyte function.

Downloaded from jpet.aspetjournals.org at ASPET Journals on April 24, 2024

JPET Fast Forward. Published on January 6, 2017 as DOI: 10.1124/jpet.116.238436
This article has not been copyedited and formatted. The final version may differ from this version.

INTRODUCTION

Signal processing in response to chemoattractant-stimulated activation of cognate seven transmembrane-span receptors (7-TMR) is a key event in regulating leukocyte behavior. Effective signal integration in leukocytes requires appropriate regulation of signal transfer from receptor to G-protein and G-protein to effector to allow cells to process and prioritize incoming signals and provide flexibility to adapt to a changing environment. Leukocyte migration and functional capacity as part of the immune response is tightly regulated by chemokines and other chemoattractants, which signal via Gαi-coupled GPCRs. Gαi in particular plays critical roles in regulating leukocyte migration and response to infection (for example, (Pero et al., 2007; Zarbock et al., 2007; Wiege et al., 2013). The mechanisms regulating chemokine and chemoattractant-stimulated responses of leukocytes are key to understanding signal processing during inflammation and immune challenge, and the identification and characterization of entities that modulate leukocyte responsiveness are of great interest and importance to the field as well as providing novel targets for potential therapeutic manipulation.

Accessory proteins for heterotrimeric G-protein signaling systems play integral roles in processing signals emanating from cell surface 7TM receptors. One family of accessory proteins includes the Group II Activator of G-protein Signaling (AGS) proteins, which were identified in a yeast-based functional screen for entities which activated heterotrimeric G-proteins in the absence of a cell surface receptor (Cismowski et al., 1999; Takesono et al., 1999). Group II AGS proteins, including AGS3/G-protein signaling modulator 1 (Gpsm1) and AGS4/Gpsm3, are characterized by the presence of at least one G-protein regulatory (GPR) motif, which bind Gαi-GDP in the absence of Gβγ.

Group II AGS proteins have shown a surprising diversity of regulatory functions. AGS3 is involved in a number of biological functions in addition to asymmetric cell division, including addiction (Bowers et al., 2004; Yao et al., 2005; Yao et al., 2006; Bowers et al., 2008), polycystic kidney disease

Downloaded from jpet.aspetjournals.org at ASPET Journals on April 24, 2024

JPET Fast Forward. Published on January 6, 2017 as DOI: 10.1124/jpet.116.238436
This article has not been copyedited and formatted. The final version may differ from this version.

and response to renal ischemia reperfusion injury (Nadella et al., 2010; Regner et al., 2011; Kwon et al., 2012), cardiovascular regulation (Blumer et al., 2008; Chauhan et al., 2012), lysosomal biogenesis and bacterial infection (Vural et al., 2015), and chemokine signal processing including leukocyte chemotaxis (Kamakura et al., 2013; Branham-O'Connor et al., 2014; Singh et al., 2014). The immune system in particular requires dynamic signal processing and spatially integrated G-protein signaling including the use of accessory proteins (e.g. (Moratz et al., 2000; Moratz et al., 2004; Han et al., 2005; Han et al., 2006; Hwang et al., 2013; Boularan and Kehrl, 2014; Branham-O'Connor et al., 2014; Huang et al., 2014; Boularan et al., 2015; Hwang et al., 2015). AGS4 (gene name: G-protein signaling modulator 3 (Gpsm3)) contains three GPR motifs and is of particular interest due to its predominant expression in the immune system ((Giguere et al., 2013), *vide infra*) where its expression appears to be responsive to external stimuli[1] and has been linked to autoimmune and inflammatory diseases (Nakou et al., 2008; Ahn et al., 2012; Kiliszek et al., 2012; Yan et al., 2012; Zhong et al., 2012; Kupfer et al., 2013).

We previously demonstrated that the Gαi-AGS4/Gpsm3 interaction is regulated by a cell surface 7TMR (Oner et al., 2010b; Robichaux et al., 2015), thus providing an alternative mode of input to heterotrimeric G-proteins, which may compliment and/or extend canonical receptor – G-protein – effector signaling systems. However, regulation of Gαi-AGS4 complex by chemokine receptors and the functional consequence of such regulation and its impact on chemokine-regulated G-protein signal processing is unknown. As part of an expanded approach to define the functional roles of AGS4/Gpsm3 *in vivo*, we utilized AGS4/Gpsm3-null mice with an initial investigation into the role of AGS4 in chemoattractant signal processing. Our data indicate that AGS4/Gpsm3 plays an important role in processing signals emanating from chemoattractant receptors that regulate leukocyte motility, thus further expanding the functional roles of G-protein signal modulators in the immune system.

MATERIALS AND METHODS

Downloaded from jpet.aspetjournals.org at ASPET Journals on April 24, 2024

JPET Fast Forward. Published on January 6, 2017 as DOI: 10.1124/jpet.116.238436
This article has not been copyedited and formatted. The final version may differ from this version.

Materials – Pertussis toxin, β-actin antibody (A5441), lipopolysaccharides (LPS) from *E. coli* 0111:B4 (L4391), N-Formyl-Met-Leu-Phe (fMLP) (F3506), AMD3100 (plerixafor), pertussis toxin and thioglycollate broth (USP Alternative, 70157) were purchased from Sigma-Aldrich (St. Louis, MO). Recombinant mouse GM-CSF, CXCL12 and CCL19 were obtained from BioAbChem Inc. (Ladson, SC). AGS4 antibody (AP5725c), anti-phospho-ERK (Tyr^{402}), and total ERK were purchased from Abgent (San Diego, CA), Santa Cruz Biotechnology (Dallas, TX) and Abcam (Cambridge, MA), respectively. Protease inhibitor cocktail tablets (Complete Mini) were obtained from Roche Applied Science. ACK Lysing Buffer (0.15 M NH_4Cl/ 0.01M $KHCO_3$/10 μM EDTA, 10-548E) was obtained from Lonza (Basel, Switzerland) and Percoll™ (17-089-02) from GE Healthcare Life Sciences (Pittsburgh, PA). Dynabeads® Untouched™ Mouse T Cells kit (11413D) was purchased from Invitrogen Life Technologies (Grand Island, NY). Corning HTS Transwell®-96 well plates (09-761-83) as well as other materials and media for cell culture were obtained from Fisher Scientific (Waltham, MA). Conjugated antibodies FITC-CD11b (557396), isotype FITC-Rat IgG2a,κ (553929), PE-Ly-6G (551461), and isotype PE-Rat IgG2b,κ (553989) were purchased from BD Biosciences (San Jose, CA). pcDNA3::CXCR4 and pIRES-puro-CXCR4-Venus were kind gifts from Dr. Michel Bouvier (University of Montreal, ON, CA) (Hamdan et al., 2006). Other materials were obtained as described elsewhere (Oner et al., 2010a; Oner et al., 2010b; Oner et al., 2013; Branham-O'Connor et al., 2014; Robichaux et al., 2015).

Bioluminescence resonance energy transfer (BRET) – BRET experiments were performed in HEK 293 cells as previously described (Oner et al., 2010b; Oner et al., 2013). Briefly, 1 x 10^6 cells were plated per well in a 6-well plate the day prior to transfection with 2 ng phRLucN3::AGS4 or AGS4-Q/A and 500 ng pcDNA3::Gαi2-YFP, 500 ng pcDNA3.1::CXCR4, 750 ng pIRES-puro-CXCR4-Venus and/or 750 ng pcDNA3::Gαi2 as indicated in the figure or figure legend using polyethyleneimine as described (Oner et al., 2010b; Oner et al., 2013). Empty pcDNA3 was used to bring the total amount of DNA used per transfection to 1.5 μg. Forty-eight hours after cell transfection, cells were dispensed in triplicate at 1 x

Downloaded from jpet.aspetjournals.org at ASPET Journals on April 24, 2024

JPET Fast Forward. Published on January 6, 2017 as DOI: 10.1124/jpet.116.238436
This article has not been copyedited and formatted. The final version may differ from this version.

10^5 cells/well in gray 96-well Optiplates (Perkin Elmer (Waltham, MA). Fluorescence and luminescence signals were measured using a TriStar LB 941 plate reader (Berthold Technologies) with MikroWin 2000 software. Cells were incubated with the CXCR4 agonist CXCL12 (10 μM) or vehicle (Tyrode's solution: 140 mM NaCl, 5 mM KCl, 1 mM $MgCl_2$, 1 mM $CaCl_2$, 0.37 mM NaH_2PO_4, 24 mM $NaHCO_3$, 10 mM (4-(2-hydroxyethyl)-1-piperazineethanesulfonic acid (HEPES), pH 7.4 and 0.1% glucose (w/v)) for 5 minutes prior to addition of coelenterazine H. Coelenterazine H (Nanolight Technology, 5 μM final concentration) was added to each well and luminescence measured after two minutes (donor: 480 + 20 nm; acceptor: 530 + 20 nm) with the TriStar LB 941 plate reader. BRET signals were determined by calculating the ratio of the light intensity emitted by the YFP divided by the light intensity emitted by Rluc. Net BRET values were determined by first calculating the 530 ± 20:480 ± 20 nm ratio and then subtracting the background BRET signal determined from cells transfected with the donor plasmid phRLucN3::AGS4 alone.

Mouse models – $Gpsm3^{-/-}$ mice generated in the C57BL/6 background were obtained through the Knockout Mouse Project (KOMP) consortium (strain $Gpsm3^{tm1(KOMP)Wtsi}$; http://www.mousephenotype.org/data/alleles/MGI:2146785/tm1%28KOMP%29Wtsi). Details on the targeting vector can be found at https://www.i-dcc.org/imits/targ_rep/alleles/12506/vector-image). Briefly, 5' and 3' homology arms (6260bp comprising exon 1 of Gpsm3 and surrounding regions and 4155bp, consisting of Gpsm3 exon 4 and surrounding regions, respectively) flanking a floxed neomycin-resistance cassette and promotorless lacZ was inserted into genomic Gpsm3 by homologous recombination. Genotyping of mice was performed with a three-primer polymerase chain reaction (PCR) design using a forward primer from the 5' end of the first exon of Gpsm3 (mgGpsm3 16651 forward), a second forward primer which is specific to the targeting plasmid (Common 3' forward), and a reverse primer from Gpsm3 exon 4 of the Gpsm3 coding sequence ("CSD-Gpsm3-SR1"). The primer sequences are as follows: mgGpsm3 16651 forward primer 5'-TGA CGG GTG GAC ACA GGA GAC TTG GGA AAG-3'; Common 3' forward (universal RAF5 forward) 5'-CAC ACC TCC CCC TGA ACC TGA AA-

Downloaded from jpet.aspetjournals.org at ASPET Journals on April 24, 2024

JPET Fast Forward. Published on January 6, 2017 as DOI: 10.1124/jpet.116.238436
This article has not been copyedited and formatted. The final version may differ from this version.

3'; CSD-Gpsm3-SR1 5'-CAG GGA AAG TGG GTG GTA AAT ACA G-3'. Using this strategy, a 1200bp band representing wild-type Gpsm3 would result from priming from mgGpsm3 16651 forward and CSD-Gpsm3-SR1, and a 776bp band representing the Gpsm3-null allele would result from priming of Common 3' forward and CSD-Gpsm3-SR1 (Figure 2A). Wild-type and $Gpsm3^{-/-}$ female littermates at 6-12 weeks of age generated from $Gpsm3^{+/-}$ intercrosses were used. Tissues and lysates were prepared and processed for immunoblotting as described (Blumer et al., 2002).

Complete Blood Count Analysis – Cardiac puncture was administered to euthanized WT or $Gpsm3^{-/-}$ mice using a 1 ml syringe fitted with a 21G needle to harvest fresh blood from the left ventricle slowly to prevent cardiac collapse of the heart and subsequently collected in BD Microtainer tubes containing EDTA. Samples were maintained at constant temperature and humidity throughout processing and analysis. Complete blood cell counts (CBCs) were performed using a HemaVet 950 (Drew Scientific, Dallas, TX) instrument to measure leukocyte, erythrocyte, and thrombocyte levels in each sample. Machine calibration and performance were verified each day that samples were analyzed using MULTI-TROL standard solution (Dog, Drew Scientific, Dallas, TX). All samples were run within 2 hr of initial collection.

Primary cells – To isolate dendritic cells, bone marrow was isolated from WT or $Gpsm3^{-/-}$ mouse femurs and tibiae using a 25G syringe to flush the bone marrow out with 10 mL of DPBS (PBS, Ca^{++} and Mg^{++} free). Isolated bone marrow was then filtered through a 40-µm nylon cell strainer, centrifuged at 4°C 500 x g and decanted. Red blood cells were lysed with 5 mL of ice-cold ACK lysis buffer (0.17 M NH_4Cl/0.17 M Tris) for 5 min at room temperature, followed by an additional spin at 4°C 500 x g to pellet the harvested bone-marrow cells. Isolated cells were then resuspended in 10 mL DC I media (RPMI-1640 supplemented with 10% FBS, 100 U/mL penicillin, 100 mg/mL streptomycin, and 20 ng/ml rmGM-CSF), and plated 4-5 x 10^5 cells/mL in a 10 cm tissue culture dish. On day four, 10 mL fresh DC I media was added to each dish. On day eight, non-adherent and loosely adherent cells were harvested, centrifuged 4°C 500 x g, decanted and re-seeded in 10 mL fresh DC II media (RPMI-1640 supplemented

Downloaded from jpet.aspetjournals.org at ASPET Journals on April 24, 2024

JPET Fast Forward. Published on January 6, 2017 as DOI: 10.1124/jpet.116.238436
This article has not been copyedited and formatted. The final version may differ from this version.

with 10% FBS, 100 U/mL penicillin, 100 mg/mL streptomycin, and 10 ng/ml rmGM-CSF) to generate immature dendritic cells (iDC). Day nine cells were treated with or without 200 ng/mL LPS for the indicated times or for 24 hours to generate mature dendritic cells (mDC). To isolate splenic B- and T-lymphocytes, spleens of WT or Gpsm3$^{-/-}$ mice were gently crushed between frosted glass slides in 10 mL serum-free RPMI. Spleen homogenate was centrifuged at 4°C 500 x g and decanted. Red blood cells were lysed with 10 mL of ice-cold ACK lysing buffer for 5 min at room temperature, followed by an additional spin at 4°C 500 x g to pellet the splenocytes. Splenocytes were then washed once and resuspended in DPBS supplemented with 0.1% BSA and 2 mM EDTA at 5 x 10^7 cells/mL or 1 x 10^8 cells/ml for subsequent B or T cell isolation, respectively. Cell isolation was performed according to Invitrogen Dynabeads protocol for untouched B cell isolation or negative T cell isolation. For neutrophil isolation, bone marrow was isolated from WT or Gpsm3$^{-/-}$ mouse femurs and tibiae using a 25G syringe to flush the bone marrow out with 10 mL of DPBS. Isolated bone marrow was then filtered through a 40-μm nylon cell strainer, centrifuged at 4°C 500 x g and decanted. Pelleted cells were resuspended in 2 mL DPBS followed by subsequent careful layering on top a 3-layer Percoll™ density gradient. The density gradient was generated by diluting 100% Percoll™ in DPBS to required densities represented by 78%, 64%, 52% Percoll dilutions. Stacking of the different layers was conducted as follows, 3 mL 78% Percoll, 2 mL 64% Percoll, and 2 mL 52% Percoll followed by subsequent 2 mL of sample. After centrifugation, 1500 x g for 40 min at 4°C, the 78/64% Percoll interface was carefully isolated and added to 9 mL of DPBS to disrupt the remaining gradient. Isolated cells were then centrifuged 4°C, 1500 x g for 5 min, decanted, and subjected to 1 mL of ice-cold ACK lysis buffer for 5 min at room temperature to remove any remaining red blood cells. Cells were then resuspended in 1-2 mL phenol red-free RPMI supplemented with 0.1% BSA and 2mM EDTA.

Immunoblotting – Single-cell suspensions from spleen were prepared by crushing freshly dissected tissues between frosted glass slides in 10 mL DPBS. After centrifugation 4°C 500 x g 5 min, samples were decanted and red blood cells lysed with 10 mL ice-cold ACK lysis buffer for 5 min at room

Downloaded from jpet.aspetjournals.org at ASPET Journals on April 24, 2024

JPET Fast Forward. Published on January 6, 2017 as DOI: 10.1124/jpet.116.238436
This article has not been copyedited and formatted. The final version may differ from this version.

temperature followed a second round of centrifugation at 4°C 500 x g for 5 min. ACK lysis buffer was then decanted and pellets were resuspended in 100-300 µL 1% NP40 lysis buffer (50 mM Tris, pH 8.0, 150 mM NaCl, 5 mM EDTA, 1% Nonidet P-40) with protease inhibitors. Samples were incubated on ice for 20 min followed by centrifugation at 10,000 x g for 30 min at 4°C. Primary cultures of dendritic cells were harvested using cell scrappers and neutrophils were collected after Percoll density centrifugation to be processed in the 1% NP-40 lysis buffer with protease inhibitors as described above. Protein concentration was determined by a Pierce BCA protein assay. Protein samples were subjected to sodium dodecyl sulfate polyacrylamide gel electrophoresis (SDS-PAGE, 10-13.5%), then separated proteins were transferred to polyvinylidene difluoride (PVDF) membranes for immunoblotting as described (Blumer et al 2002). Immunoblotting with AGS4 antibodies (Abgent, San Diego, CA) was conducted as follows: Membranes were then blocked with 50% Odyssey Buffer [LI-COR Biosciences] and 50% Tris-buffered saline + 0.01% Tween (TBST) for 30 min at room temperature, incubated with AGS4 antibody (1:250 dilution) overnight 4°C, followed by three 10 min washes in TBST. Membranes were then exposed to 1:5,000 dilution of horseradish peroxidase-conjugated goat anti-rabbit IgG 30 min room temperature, followed by three 30 min washes with TBST and subsequent exposure with ECL.

Phospho-ERK (pERK) assays – Single cell suspensions of WT and Gpsm3$^{-/-}$ cultured dendritic cells or freshly isolated spelenocytes were isolated as described above. Cells were stimulated in the absence or presence of 200 ng/mL CXCL12, a concentration based on our previous experience with primary dendritic cell cultures and splenocytes (Branham-O'Connor et al., 2014) and that of others (Basu and Broxmeyer, 2005; Petit et al., 2005; Basu and Broxmeyer, 2009; Dorner et al., 2009; Boudot et al., 2014), for 0.5, 2 and 5 minutes. At the indicated times, cells were immediately lysed in 1% NP40 buffer with protease inhibitors and additional phosphatase inhibitors (50 mM NaF, 5 mM sodium pyrophosphate, 40 mM β-glycerophosphate and 200 µM Na_3VO_4) on ice for 20 min followed by centrifugation at 10,000 x g for 30 min at 4°C. Samples were subjected to SDS-PAGE, proteins transferred to PVDF membranes and immunoblotted for anti-phospho-Erk (Y402) (Santa Cruz

Downloaded from jpet.aspetjournals.org at ASPET Journals on April 24, 2024

JPET Fast Forward. Published on January 6, 2017 as DOI: 10.1124/jpet.116.238436
This article has not been copyedited and formatted. The final version may differ from this version.

Biotechnology, Dallas, TX, USA), or total Erk (Abcam, Cambridge, MA, USA) antibodies. Densitometric quantification of the immunoblotted bands was performed using ImageJ densitometry software (Version 1.49i, National Institutes of Health, Bethesda, MD). Selected bands were quantified based on their relative intensities and normalized to total Erk.

Chemotaxis – Corning Transwell 24-well inserts (6.5 mm diameter, 5.0 μm pore size) or 96-well inserts (5.0 μm pore size) were used for all chemotaxis assays. For dendritic cell chemotaxis, 235 μL of serum-free RPMI with or without CXCL12 (10-500 ng/mL) or CCL19 (250 ng/mL) was added to each lower chamber and 75 μL of approximately 3 x 10^6 cells/ml were loaded into the upper chambers. For T-lymphocytes, 235 μL of serum-free RPMI supplemented with 0.1% BSA and 2mM EDTA with or without CCL19 (50-300 ng/ml) was added to each lower chamber, and 75 μL of approximately 1 x 10^7 lymphocytes/mL were added into the upper chambers. For neutrophils, 235 μL of serum-free RPMI supplemented with 0.1% BSA and 2mM EDTA with or without fMLP (0.1-5.0 μM) was added to each lower chamber, and 75 μL of approximately 5 x 10^6 cells/ml were added to the upper chambers. Chemotaxis chambers were incubated at 37°C, 5% CO_2 for 20 hrs for dendritic cells, 5 hrs for lymphocytes, and 3 hrs for neutrophils. The upper chamber was removed and cells migrating to the bottom chamber as well as cells retained in the upper chamber were counted by flow cytometry. The percentage of cells migrated was calculated relative to the input, where the number of cells migrating to the bottom chamber in the absence of chemokine was subtracted. Chemotaxis data shown are the means +/- SE from at least three independent experiments, each containing at least triplicate determinations.

Thioglycollate-induced intraperitoneal inflammation – WT and Gpsm3$^{-/-}$ mice received intraperitoneal injections using an insulin syringe (28G) to deliver 1 mL of DPBS or 4% thioglycollate (in DPBS, sterilized, and aged for a minimum of 2 wks). After 2 hrs, mice were euthanized and intraperitoneal (IP) cavity lavage was carried out through injection of 10 mL cold DPBS and thorough subsequent agitation of the cavity. Blood (350 – 600 μL) was also collected by cardiac puncture and bone marrow was collected from femurs as described above in Primary Cells section. Isolated cells were centrifuged 4°C

Downloaded from jpet.aspetjournals.org at ASPET Journals on April 24, 2024

JPET Fast Forward. Published on January 6, 2017 as DOI: 10.1124/jpet.116.238436
This article has not been copyedited and formatted. The final version may differ from this version.

500 x g 5 min, excess supernatant decanted, and red blood cells were lysed using 1 mL ice-cold ACK lysis buffer (5 min incubation followed by subsequent 500 x g centrifugation for 5 min). Blood samples required a minimum of two ACK lysis steps to remove all of the red blood cells. Isolated IP lavage cells were then resuspended in 50 µL of PBS with 1% BSA and 0.1% NaN_3 (PBS-BSA), isolated cells from the blood were resuspended in 200 µL of PBS-BSA, and isolated bone marrow cells were resuspended in 1 mL of PBS-BSA. Each sample then had 50 µL subjected to incubation with conjugated antibodies for analysis by flow cytometry as described below.

Flow cytometry and cell sorting – Single-cell suspensions of WT and $Gpsm3^{-/-}$ neutrophils collected from Percoll density centrifugation or from thioglycollate-induced inflammation experiments were prepared as described above. Cell pellets were washed and resuspended in 50 µL PBS supplemented with 1% BSA and 0.1% NaN_3 (PBS-BSA). Cells were incubated with primary FITC-CD11b (0.3 µL, 0.15 µg) or PE-Ly-6G (2 µL, 0.4 µg) conjugated Abs or isotype controls FITC-Rat IgG2a,κ (1 µL, 0.5 µg) or PE-Rat IgG2b,κ (3 µL,0.6 µg) in PBS-BSA for 30 min at 4°C (BD Pharmingen, San Diego, CA). Cells were washed thrice with 500 µL PBS-BSA with subsequent centrifugations 4°C 500 x g 5 min, and resuspended in 250-500 µl of PBS-BSA for analysis by flow cytometer (BD Pharmingen). Neutrophil populations were observed as being dual positive ($CD11b^+$, $Ly\text{-}6G^+$).

Data Analysis – Statistical significance for differences involving a single intervention was determined by one-way analysis of variance (ANOVA) followed with a post hoc Tukey's test using GraphPad Prism version 4.03 (GraphPad Software, San Diego).

RESULTS

We previously demonstrated that the Gαi-AGS4 interaction is regulated by Gαi-coupled 7-TM receptors such as the α_2-adrenergric receptor (Oner et al., 2010b; Robichaux et al., 2015). As an initial approach to determine if such regulation of Gαi-AGS4 extends to chemokine receptors, which are widely

Downloaded from jpet.aspetjournals.org at ASPET Journals on April 24, 2024

JPET Fast Forward. Published on January 6, 2017 as DOI: 10.1124/jpet.116.238436
This article has not been copyedited and formatted. The final version may differ from this version.

expressed in the immune system and are Gαi-coupled, we used our previously established bioluminescence resonance energy transfer (BRET) platform to monitor the Gαi-AGS4 interaction in real-time in live cells (HEK 293) in response to expression and activation of a prototypical chemokine receptor, CXCR4. Activation of CXCR4 by the agonist CXCL12 significantly reduced the $G\alpha i_2$-AGS4 interaction, indicating regulation of this complex is indeed sensitive to chemokine receptor activation (Figure 1A). CXCL12 regulation of the $G\alpha i_2$-AGS4 complex required the presence of CXCR4 and was blocked by the CXCR4 antagonist AMD3100 (plerixafor) and by pertussis toxin pretreatment, which ADP-ribosylates Gαi and prevents receptor – G-protein coupling. BRET signals were completely absent with a mutant form of AGS4 in which a conserved glutamate residue in each of its three GPR motifs was mutated to alanine ("AGS4-Q/A"), rendering it incapable of binding Gαi (Cao et al., 2004; Oner et al., 2010b), which serves as an internal negative control for the system (Figure 1A).

We next sought to determine if AGS4-Gαi complexes might actually interface directly with CXCR4 in an agonist-regulated manner by modifying our BRET platform to include CXCR4-Venus as the acceptor rather than $G\alpha i_2$-YFP (Figure 1B, top panel). In the absence of co-expressed $G\alpha i_2$, AGS4 – CXCR4 BRET signals were only slightly above background; however, when $G\alpha i_2$ was co-expressed, a robust AGS4 – CXCR4 BRET signal was observed, indicating a $G\alpha i_2$-dependent tripartite complex between AGS4, $G\alpha i_2$ and CXCR4 (Figure 1B, bottom panel). This complex was also regulated by CXCL12, the affect of which was blocked by the antagonist AMD3100 (plerixafor) and pertussis toxin pretreatment (Figure 1B). Taken together, these data are consistent with our previous data (Oner et al., 2010b; Robichaux et al., 2015) and indicate that the AGS4-Gαi module is capable of forming a complex with CXCR4 that is agonist-dependent, with broad implications on chemokine signal integration.

To further understand the functional consequence of this novel regulation and as part of an ongoing effort to define the functional roles of GPR proteins in the immune system (e.g. (Branham-O'Connor et al., 2014)), AGS4/Gpsm3-null mice were used (see Materials and Methods for details).

Downloaded from jpet.aspetjournals.org at ASPET Journals on April 24, 2024

JPET Fast Forward. Published on January 6, 2017 as DOI: 10.1124/jpet.116.238436
This article has not been copyedited and formatted. The final version may differ from this version.

Genotyping and immunoblotting confirmed that the insertion of the targeting plasmid resulted in the loss of AGS4 protein expression (Figure 2A, B).

The location of the Gpsm3 gene within the Class III MHC locus suggested that AGS4/Gpsm3 is primarily expressed in the immune system, and initial observations from us and others indicated this was indeed the case (Cao et al., 2004; Kimple et al., 2004; Zhao et al., 2010; Schmidt et al., 2012; Giguere et al., 2013). We also discovered AGS4 expression in primary bone marrow-derived dendritic cells and splenocytes (Figure 2B). CBC analysis indicated that AGS4/Gpsm3-null mice exhibited a mild but significant neutropenia and lymphocytosis while other leukocyte populations were unaltered (Figure 2C).

As an initial approach to determine the role of AGS4 in G-protein signal processing in leukocytes, we examined chemokine-mediated activation of ERK1/2 in primary dendritic cells and splenocytes. Loss of AGS4/Gpsm3 expression resulted in a reduction in CXCL12-activated ERK1/2 phosphorylation in both populations of cells (Figure 3), suggesting a role for AGS4 in chemokine signal processing.

In conjunction with the known role of Gαi-based signaling in chemotaxis (e.g. (Rudolph et al., 1995; Han et al., 2005; Hwang et al., 2007; Zarbock et al., 2007; Cho et al., 2012; Wiege et al., 2012; Surve et al., 2016), previous reports also indicate that ERK1/2 activation subsequent to chemokine receptor stimulation plays an important role in directed migration of leukocytes (Tilton et al., 2000; Delgado-Martin et al., 2011; Sagar et al., 2012). To explore the possible role of AGS4/Gpsm3 in chemotaxis, we measured chemokine-directed migration in primary dendritic cells and T lymphocytes. We observed ~25% reductions in CXCL12-directed chemotaxis in primary dendritic cells and CCL19-directed chemotaxis in primary T lymphocytes from AGS4/Gpsm3-null mice compared to WT mice (Figure 4A,B). There were no significant differences in random migration of primary dendritic cells and T lymphocytes from AGS4/Gpsm3-null and WT mice, indicating that the chemotactic defects in AGS4/Gpsm3-null mice was primarily directional and not due to an overall increase in migratory capacity.[2] In addition, flow cytometry analysis revealed that chemokine receptor levels were unaltered in

Downloaded from jpet.aspetjournals.org at ASPET Journals on April 24, 2024

JPET Fast Forward. Published on January 6, 2017 as DOI: 10.1124/jpet.116.238436
This article has not been copyedited and formatted. The final version may differ from this version.

leukocytes from AGS4/Gpsm3-null mice, thus indicating that the chemotactic defects observed were not due to the loss of chemokine receptor expression.[3]

Gene expression databases indicate that AGS4 is highly expressed in neutrophils (Heng and Painter, 2008; Database, 2014), and indeed, we observed high levels of AGS4 expression in primary mouse neutrophils (Figure 5A). Therefore, we measured chemotactic responses in primary neutrophils from WT and AGS4/Gpsm3-null mice, and observed significant defects in AGS4/Gpsm3-null neutrophil chemotaxis to fMLP (Figure 5B). Interestingly, the chemotactic defect observed was dose-dependent, with a ~60% reduction in directed migration to the highest dose of agonist (Figure 5B), suggesting AGS4/Gpsm3 may play a role in shaping cell responses at high levels of receptor activation. We next asked if the requirement of AGS4/Gpsm3 for proper neutrophil chemotaxis *ex vivo* was also observed *in vivo*. As an initial approach to address this question, we used an induced peritonitis model by intraperitoneal injection of thioglycollate to measure the recruitment of neutrophils to the site of inflammation. While induced peritonitis resulted in a significant accumulation of WT neutrophils in the IP cavity, the level of AGS4/Gpsm3-null neutrophils recruited to the IP cavity was reduced by ~80% (Figure 5C, left panel). Levels of neutrophils in the blood and bone marrow were not different between WT and AGS4/Gpsm3-null mice (Figure 5C, center and right panels). These data suggest a possible deficiency in extravasation or a tardive response in AGS4/Gpsm3-null neutrophils.

DISCUSSION

A growing number of cellular and physiological roles have been ascribed to GPR proteins in systems where signal modulation and adaptation are critical for system responsiveness (Bowers et al., 2004; Yao et al., 2005; Yao et al., 2006; Blumer et al., 2008; Bowers et al., 2008; Nadella et al., 2010; Regner et al., 2011; Chauhan et al., 2012; Kwon et al., 2012; Giguere et al., 2013; Kamakura et al., 2013; Branham-O'Connor et al., 2014; Singh et al., 2014). The immune system is certainly an area rich in signaling modulation and adaptation and requires dynamic signal processing and spatially integrated G-

Downloaded from jpet.aspetjournals.org at ASPET Journals on April 24, 2024

JPET Fast Forward. Published on January 6, 2017 as DOI: 10.1124/jpet.116.238436
This article has not been copyedited and formatted. The final version may differ from this version.

protein signaling (Cho and Kehrl, 2009; Kehrl et al., 2009). Indeed, G-proteins and accessory proteins such as RGS proteins play critical roles in signal processing in the immune system (Rudolph et al., 1995; Huang et al., 2003; Han et al., 2005; Skokowa et al., 2005; Han et al., 2006; Hwang et al., 2007; Pero et al., 2007; Zarbock et al., 2007; Cho and Kehrl, 2009; Kehrl et al., 2009; Cho et al., 2012; Wiege et al., 2012; Wiege et al., 2013; Surve et al., 2014; Rangel-Moreno et al., 2016; Surve et al., 2016).

Alterations in circulating populations of neutrophils and lymphocytes in AGS4/Gpsm3-null mice may suggest a defect either in the production or differentiation of these cells or a defect in their egress from the bone marrow into the circulation. Interestingly, similar phenotypes including mild neutropenia and a defect in neutrophil migration were also observed in mice with an RGS-insensitive Gnai2 knock-in allele (Cho et al., 2012), suggesting that regulation of the duration of G-protein signaling subsequent to chemoattractant exposure is critical in neutrophil mobility and recruitment to sites of inflammation.

Our initial approach to investigating the role of AGS4 in chemokine signal processing reported in this manuscript utilized key prototype chemokine and chemoattractant receptors. AGS4 may possess selectivity for modulating G-protein signal processing for different chemokine receptors and this is the basis for future studies. We have shown here that AGS4 forms a Gαi-dependent complex with the chemokine receptor CXCR4 that is regulated by agonist (Figure 1). Based on data presented here and elsewhere, this agonist regulation is likely due to the apparent coupling of the Gαi-AGS4 complex directly with the agonist-bound GPCR (Robichaux et al., 2015). While our data indicate defective chemokine signal integration from CXCR4 activation upon loss of AGS4 expression in dendritic cells and lymphocytes, we cannot rule out a potential role for CXCR7, which can also bind CXCL12. However, CXCR7-mediated responses to CXCL12 are G-protein independent (Burns et al., 2006; Zabel et al., 2009; Rajagopal et al., 2010), thus likely limiting the direct involvement of G-protein modulators like AGS4 in CXCLX12/CXCR7-mediated signaling. There are also reports of potential CXCR4-CXCR7 dimerization (Levoye et al., 2009; Decaillot et al., 2011); thus the interplay between these two receptors and the influence AGS4 may have on such a complex may be of future interest.

Downloaded from jpet.aspetjournals.org at ASPET Journals on April 24, 2024

JPET Fast Forward. Published on January 6, 2017 as DOI: 10.1124/jpet.116.238436
This article has not been copyedited and formatted. The final version may differ from this version.

We previously demonstrated that the Gαi-GPR module can be regulated by a 7TMR (Oner et al., 2010a; Oner et al., 2010b; Robichaux et al., 2015). Recently, we reported that this regulation reflects a direct engagement of Gαi-GPR with the 7TMR analogous to canonical Gαβγ. It is possible that direct input from chemoattractant receptors to the Gαi-AGS4 module may play an important modulatory role in chemokine signal processing, and the loss of this alternative mode of signal input to Gαi signaling may be responsible for the defects observed in AGS4/Gpsm3-null leukocytes. Such regulation would be a novel mechanism for G-protein signal processing, as Gαi-specific roles in chemoattractant signal processing have been elusive. However, there are reports suggesting Gαi-specific functions in leukocyte responses to chemokines (Surve et al., 2016). While Gβγ is generally considered the primary G-protein signaling unit within leukocytes (Arai et al., 1997; Neptune and Bourne, 1997; Peracino et al., 1998; Lehmann et al., 2008; Zhang et al., 2010), (e.g. elevations in intracellular Ca^{2+}, activation of PI3Kγ and downstream activation of small GTPases required for directed migration) Surve *et al.* (Surve et al., 2016) recently reported that Gαi signaling in leukocytes appears to be required to locally counteract Gβγ-mediated increases in cAMP to facilitate cell polarity and directed migration. We speculate that the Gαi-AGS4 module, and perhaps Gαi-AGS3 complexes as well (Blumer and Lanier, 2014; Branham-O'Connor et al., 2014; Robichaux et al., 2015), by coupling directly with chemokine receptors, may increase the available pool of Gαi-GTP to assist in dampening local cAMP levels to facilitate leukocyte polarity and directed migration.

Within the immune system, AGS4 is highly expressed in neutrophils (Fig. 5), perhaps higher than any other immune cell type (Heng and Painter, 2008; Database, 2014), which suggests an important role for AGS4 in neutrophils and also provides an attractive model for studying the role of AGS4 in the innate immune system. The apparent dose-dependent chemotactic defect observed in AGS4/Gpsm3-null neutrophils (Figure 5B) suggests that AGS4 may play an important role in modulating cellular responses at higher levels of receptor activation. Similar observations were noted for regulator of G-protein signaling 1 (RGS1), another accessory protein important for chemokine-regulated G-protein signal

Downloaded from jpet.aspetjournals.org at ASPET Journals on April 24, 2024

JPET Fast Forward. Published on January 6, 2017 as DOI: 10.1124/jpet.116.238436
This article has not been copyedited and formatted. The final version may differ from this version.

processing (Han et al., 2006; Hwang et al., 2010). Furthermore, our data indicate that AGS4-null neutrophils have a defect in chemoattractant-mediated migration *ex vivo*, which manifests in a defect in neutrophil recruitment to sites of inflammation *in vivo* (Fig. 5). It is interesting to note that either inhibition or loss of $G\alpha i_2$ expression in leukocytes and endothelial cells also impairs neutrophil extravasation to sites of inflammation (Warnock et al., 1998; Pero et al., 2007; Zarbock et al., 2007; Wiege et al., 2012). Thus, aberrant transmigration of AGS4/Gpsm3-null neutrophils from the blood to the IP cavity may reflect simultaneous aberrant $G\alpha i_2$ signaling in both neutrophils and endothelial cells, which together contribute to the observed defects in innate immunity. Future studies are aimed at validating these results in primary human leukocytes. Taken together, these data suggest that AGS4 may play a role in the inflammatory response and that the AGS4 – Gαi module may be an attractive target for the development of potential therapeutics.

Downloaded from jpet.aspetjournals.org at ASPET Journals on April 24, 2024

JPET Fast Forward. Published on January 6, 2017 as DOI: 10.1124/jpet.116.238436
This article has not been copyedited and formatted. The final version may differ from this version.

ACKNOWLEDGEMENTS

We thank Ellen Maher, Christine Webster and Hunter Matthews for expert technical assistance. We thank Dr. Michel Bouvier (University of Montreal, Montreal, ON, CA) for generously providing CXCR4 and CXCR4-Venus expression plasmids. J.B.B. would also like to thank Dr. Stephen Lanier (Wayne State University) for helpful discussions and support.

AUTHORSHIP CONTRIBUTIONS

Participated in research design: Robichaux, Branham-O'Connor, Hwang, Vural, Kehrl, Blumer

Conducted experiments: Robichaux, Branham-O'Connor, Hwang, Vural, Kehrl, Blumer

Contributed new reagents or analytic tools: Robichaux, Branham-O'Connor, Hwang, Vural, Kehrl, Blumer

Performed data analysis: Robichaux, Branham-O'Connor, Hwang, Vural, Kehrl, Blumer

Wrote or contributed to the writing of the manuscript: Robichaux, Branham-O'Connor, Vural, Kehrl, Blumer

Downloaded from jpet.aspetjournals.org at ASPET Journals on April 24, 2024

JPET Fast Forward. Published on January 6, 2017 as DOI: 10.1124/jpet.116.238436
This article has not been copyedited and formatted. The final version may differ from this version.

LITERATURE CITED

Ahn R, Ding YC, Murray J, Fasano A, Green PH, Neuhausen SL and Garner C (2012) Association analysis of the extended MHC region in celiac disease implicates multiple independent susceptibility loci. *PLoS One* **7**:e36926.

Arai H, Tsou CL and Charo IF (1997) Chemotaxis in a lymphocyte cell line transfected with C-C chemokine receptor 2B: evidence that directed migration is mediated by betagamma dimers released by activation of Galphai-coupled receptors. *Proc Natl Acad Sci U S A* **94**:14495-14499.

Basu S and Broxmeyer HE (2005) Transforming growth factor-{beta}1 modulates responses of CD34+ cord blood cells to stromal cell-derived factor-1/CXCL12. *Blood* **106**:485-493.

Basu S and Broxmeyer HE (2009) CCR5 ligands modulate CXCL12-induced chemotaxis, adhesion, and Akt phosphorylation of human cord blood CD34+ cells. *J Immunol* **183**:7478-7488.

Blumer JB, Chandler LJ and Lanier SM (2002) Expression analysis and subcellular distribution of the two G-protein regulators AGS3 and LGN indicate distinct functionality. Localization of LGN to the midbody during cytokinesis. *J Biol Chem* **277**:15897-15903.

Blumer JB and Lanier SM (2014) Activators of G protein signaling exhibit broad functionality and define a distinct core signaling triad. *Mol Pharmacol* **85**:388-396.

Blumer JB, Lord K, Saunders TL, Pacchioni A, Black C, Lazartigues E, Varner KJ, Gettys TW and Lanier SM (2008) Activator of G protein signaling 3 null mice: I. Unexpected alterations in metabolic and cardiovascular function. *Endocrinology* **149**:3842-3849.

Boudot A, Kerdivel G, Lecomte S, Flouriot G, Desille M, Godey F, Leveque J, Tas P, Le Drean Y and Pakdel F (2014) COUP-TFI modifies CXCL12 and CXCR4 expression by activating EGF signaling and stimulates breast cancer cell migration. *BMC Cancer* **14**:407.

Downloaded from jpet.aspetjournals.org at ASPET Journals on April 24, 2024

JPET Fast Forward. Published on January 6, 2017 as DOI: 10.1124/jpet.116.238436
This article has not been copyedited and formatted. The final version may differ from this version.

Boularan C, Hwang IY, Kamenyeva O, Park C, Harrison K, Huang Z and Kehrl JH (2015) B Lymphocyte-Specific Loss of Ric-8A Results in a Galpha Protein Deficit and Severe Humoral Immunodeficiency. *J Immunol* **195**:2090-2102.

Boularan C and Kehrl JH (2014) Implications of non-canonical G-protein signaling for the immune system. *Cell Signal* **26**:1269-1282.

Bowers MS, Hopf FW, Chou JK, Guillory AM, Chang SJ, Janak PH, Bonci A and Diamond I (2008) Nucleus accumbens AGS3 expression drives ethanol seeking through G betagamma. *Proc Natl Acad Sci U S A* **105**:12533-12538.

Bowers MS, McFarland K, Lake RW, Peterson YK, Lapish CC, Gregory ML, Lanier SM and Kalivas PW (2004) Activator of G protein signaling 3: a gatekeeper of cocaine sensitization and drug seeking. *Neuron* **42**:269-281.

Branham-O'Connor M, Robichaux WG, 3rd, Zhang XK, Cho H, Kehrl JH, Lanier SM and Blumer JB (2014) Defective Chemokine Signal Integration in Leukocytes Lacking Activator of G Protein Signaling 3 (AGS3). *J Biol Chem* **289**:10738-10747.

Burns JM, Summers BC, Wang Y, Melikian A, Berahovich R, Miao Z, Penfold ME, Sunshine MJ, Littman DR, Kuo CJ, Wei K, McMaster BE, Wright K, Howard MC and Schall TJ (2006) A novel chemokine receptor for SDF-1 and I-TAC involved in cell survival, cell adhesion, and tumor development. *J Exp Med* **203**:2201-2213.

Cao X, Cismowski MJ, Sato M, Blumer JB and Lanier SM (2004) Identification and characterization of AGS4: a protein containing three G-protein regulatory motifs that regulate the activation state of Gialpha. *J Biol Chem* **279**:27567-27574.

Chauhan S, Jelen F, Sharina I and Martin E (2012) The G-protein regulator LGN modulates the activity of the NO receptor soluble guanylate cyclase. *Biochem J* **446**:445-453.

Cho H, Kamenyeva O, Yung S, Gao JL, Hwang IY, Park C, Murphy PM, Neubig RR and Kehrl JH (2012) The loss of RGS protein-Galpha(i2) interactions results in markedly impaired mouse neutrophil trafficking to inflammatory sites. *Mol Cell Biol* **32**:4561-4571.

Downloaded from jpet.aspetjournals.org at ASPET Journals on April 24, 2024

JPET Fast Forward. Published on January 6, 2017 as DOI: 10.1124/jpet.116.238436
This article has not been copyedited and formatted. The final version may differ from this version.

Cho H and Kehrl JH (2009) Regulation of immune function by G protein-coupled receptors, trimeric G proteins, and RGS proteins. *Prog Mol Biol Transl Sci* **86**:249-298.

Cismowski MJ, Takesono A, Ma C, Lizano JS, Xie X, Fuernkranz H, Lanier SM and Duzic E (1999) Genetic screens in yeast to identify mammalian nonreceptor modulators of G-protein signaling. *Nat Biotechnol* **17**:878-883.

Database IGP (2014) Immunological Genome Project Database. *www.immgen.org*.

Decaillot FM, Kazmi MA, Lin Y, Ray-Saha S, Sakmar TP and Sachdev P (2011) CXCR7/CXCR4 heterodimer constitutively recruits beta-arrestin to enhance cell migration. *J Biol Chem* **286**:32188-32197.

Delgado-Martin C, Escribano C, Pablos JL, Riol-Blanco L and Rodriguez-Fernandez JL (2011) Chemokine CXCL12 uses CXCR4 and a signaling core formed by bifunctional Akt, extracellular signal-regulated kinase (ERK)1/2, and mammalian target of rapamycin complex 1 (mTORC1) proteins to control chemotaxis and survival simultaneously in mature dendritic cells. *J Biol Chem* **286**:37222-37236.

Dorner BG, Dorner MB, Zhou X, Opitz C, Mora A, Guttler S, Hutloff A, Mages HW, Ranke K, Schaefer M, Jack RS, Henn V and Kroczek RA (2009) Selective expression of the chemokine receptor XCR1 on cross-presenting dendritic cells determines cooperation with CD8+ T cells. *Immunity* **31**:823-833.

Giguere PM, Billard MJ, Laroche G, Buckley BK, Timoshchenko RG, McGinnis MW, Esserman D, Foreman O, Liu P, Siderovski DP and Tarrant TK (2013) G-protein signaling modulator-3, a gene linked to autoimmune diseases, regulates monocyte function and its deficiency protects from inflammatory arthritis. *Mol Immunol* **54**:193-198.

Hamdan FF, Percherancier Y, Breton B and Bouvier M (2006) Monitoring protein-protein interactions in living cells by bioluminescence resonance energy transfer (BRET). *Curr Protoc Neurosci* **Chapter 5**:Unit 5 23.

Downloaded from jpet.aspetjournals.org at ASPET Journals on April 24, 2024

JPET Fast Forward. Published on January 6, 2017 as DOI: 10.1124/jpet.116.238436
This article has not been copyedited and formatted. The final version may differ from this version.

Han JI, Huang NN, Kim DU and Kehrl JH (2006) RGS1 and RGS13 mRNA silencing in a human B lymphoma line enhances responsiveness to chemoattractants and impairs desensitization. *J Leukoc Biol* **79**:1357-1368.

Han SB, Moratz C, Huang NN, Kelsall B, Cho H, Shi CS, Schwartz O and Kehrl JH (2005) Rgs1 and Gnai2 regulate the entrance of B lymphocytes into lymph nodes and B cell motility within lymph node follicles. *Immunity* **22**:343-354.

Heng TS and Painter MW (2008) The Immunological Genome Project: networks of gene expression in immune cells. *Nat Immunol* **9**:1091-1094.

Huang NN, Becker S, Boularan C, Kamenyeva O, Vural A, Hwang IY, Shi CS and Kehrl JH (2014) Canonical and noncanonical g-protein signaling helps coordinate actin dynamics to promote macrophage phagocytosis of zymosan. *Mol Cell Biol* **34**:4186-4199.

Huang TT, Zong Y, Dalwadi H, Chung C, Miceli MC, Spicher K, Birnbaumer L, Braun J and Aranda R (2003) TCR-mediated hyper-responsiveness of autoimmune Galphai2(-/-) mice is an intrinsic naive CD4(+) T cell disorder selective for the Galphai2 subunit. *Int Immunol* **15**:1359-1367.

Hwang IY, Hwang KS, Park C, Harrison KA and Kehrl JH (2013) Rgs13 constrains early B cell responses and limits germinal center sizes. *PLoS One* **8**:e60139.

Hwang IY, Park C, Harrision KA, Huang NN and Kehrl JH (2010) Variations in Gnai2 and Rgs1 expression affect chemokine receptor signaling and the organization of secondary lymphoid organs. *Genes Immun* **11**:384-396.

Hwang IY, Park C, Harrison K, Boularan C, Gales C and Kehrl JH (2015) An essential role for RGS protein/Galphai2 interactions in B lymphocyte-directed cell migration and trafficking. *J Immunol* **194**:2128-2139.

Hwang IY, Park C and Kehrl JH (2007) Impaired trafficking of Gnai2+/- and Gnai2-/- T lymphocytes: implications for T cell movement within lymph nodes. *J Immunol* **179**:439-448.

Downloaded from jpet.aspetjournals.org at ASPET Journals on April 24, 2024

JPET Fast Forward. Published on January 6, 2017 as DOI: 10.1124/jpet.116.238436
This article has not been copyedited and formatted. The final version may differ from this version.

Kamakura S, Nomura M, Hayase J, Iwakiri Y, Nishikimi A, Takayanagi R, Fukui Y and Sumimoto H (2013) The cell polarity protein mInsc regulates neutrophil chemotaxis via a noncanonical G protein signaling pathway. *Dev Cell* **26**:292-302.

Kehrl JH, Hwang IY and Park C (2009) Chemoattract receptor signaling and its role in lymphocyte motility and trafficking. *Curr Top Microbiol Immunol* **334**:107-127.

Kiliszek M, Burzynska B, Michalak M, Gora M, Winkler A, Maciejak A, Leszczynska A, Gajda E, Kochanowski J and Opolski G (2012) Altered gene expression pattern in peripheral blood mononuclear cells in patients with acute myocardial infarction. *PLoS One* **7**:e50054.

Kimple RJ, Willard FS, Hains MD, Jones MB, Nweke GK and Siderovski DP (2004) Guanine nucleotide dissociation inhibitor activity of the triple GoLoco motif protein G18: alanine-to-aspartate mutation restores function to an inactive second GoLoco motif. *Biochem J* **378**:801-808.

Kupfer DM, White VL, Strayer DL, Crouch DJ and Burian D (2013) Microarray characterization of gene expression changes in blood during acute ethanol exposure. *BMC Med Genomics* **6**:26.

Kwon M, Pavlov TS, Nozu K, Rasmussen SA, Ilatovskaya DV, Lerch-Gaggl A, North LM, Kim H, Qian F, Sweeney WE, Jr., Avner ED, Blumer JB, Staruschenko A and Park F (2012) G-protein signaling modulator 1 deficiency accelerates cystic disease in an orthologous mouse model of autosomal dominant polycystic kidney disease. *Proc Natl Acad Sci U S A* **109**:21462-21467.

Lehmann DM, Seneviratne AM and Smrcka AV (2008) Small molecule disruption of G protein beta gamma subunit signaling inhibits neutrophil chemotaxis and inflammation. *Mol Pharmacol* **73**:410-418.

Levoye A, Balabanian K, Baleux F, Bachelerie F and Lagane B (2009) CXCR7 heterodimerizes with CXCR4 and regulates CXCL12-mediated G protein signaling. *Blood* **113**:6085-6093.

Moratz C, Hayman JR, Gu H and Kehrl JH (2004) Abnormal B-cell responses to chemokines, disturbed plasma cell localization, and distorted immune tissue architecture in Rgs1-/- mice. *Mol Cell Biol* **24**:5767-5775.

Downloaded from jpet.aspetjournals.org at ASPET Journals on April 24, 2024

JPET Fast Forward. Published on January 6, 2017 as DOI: 10.1124/jpet.116.238436
This article has not been copyedited and formatted. The final version may differ from this version.

Moratz C, Kang VH, Druey KM, Shi CS, Scheschonka A, Murphy PM, Kozasa T and Kehrl JH (2000) Regulator of G protein signaling 1 (RGS1) markedly impairs Gi alpha signaling responses of B lymphocytes. *J Immunol* **164**:1829-1838.

Nadella R, Blumer JB, Jia G, Kwon M, Akbulut T, Qian F, Sedlic F, Wakatsuki T, Sweeney WE, Jr., Wilson PD, Lanier SM and Park F (2010) Activator of G protein signaling 3 promotes epithelial cell proliferation in PKD. *J Am Soc Nephrol* **21**:1275-1280.

Nakou M, Knowlton N, Frank MB, Bertsias G, Osban J, Sandel CE, Papadaki H, Raptopoulou A, Sidiropoulos P, Kritikos I, Tassiulas I, Centola M and Boumpas DT (2008) Gene expression in systemic lupus erythematosus: bone marrow analysis differentiates active from inactive disease and reveals apoptosis and granulopoiesis signatures. *Arthritis Rheum* **58**:3541-3549.

Neptune ER and Bourne HR (1997) Receptors induce chemotaxis by releasing the betagamma subunit of Gi, not by activating Gq or Gs. *Proc Natl Acad Sci U S A* **94**:14489-14494.

Oner SS, An N, Vural A, Breton B, Bouvier M, Blumer JB and Lanier SM (2010a) Regulation of the AGS3.G{alpha}i signaling complex by a seven-transmembrane span receptor. *J Biol Chem* **285**:33949-33958.

Oner SS, Blumer JB and Lanier SM (2013) Group II activators of G-protein signaling: monitoring the interaction of Galpha with the G-protein regulatory motif in the intact cell. *Methods Enzymol* **522**:153-167.

Oner SS, Maher EM, Breton B, Bouvier M and Blumer JB (2010b) Receptor-regulated interaction of activator of G-protein signaling-4 and Galphai. *J Biol Chem* **285**:20588-20594.

Peracino B, Borleis J, Jin T, Westphal M, Schwartz JM, Wu L, Bracco E, Gerisch G, Devreotes P and Bozzaro S (1998) G protein beta subunit-null mutants are impaired in phagocytosis and chemotaxis due to inappropriate regulation of the actin cytoskeleton. *J Cell Biol* **141**:1529-1537.

Pero RS, Borchers MT, Spicher K, Ochkur SI, Sikora L, Rao SP, Abdala-Valencia H, O'Neill KR, Shen H, McGarry MP, Lee NA, Cook-Mills JM, Sriramarao P, Simon MI, Birnbaumer L and Lee JJ

Downloaded from jpet.aspetjournals.org at ASPET Journals on April 24, 2024

JPET Fast Forward. Published on January 6, 2017 as DOI: 10.1124/jpet.116.238436
This article has not been copyedited and formatted. The final version may differ from this version.

(2007) Galphai2-mediated signaling events in the endothelium are involved in controlling leukocyte extravasation. *Proc Natl Acad Sci U S A* **104**:4371-4376.

Petit I, Goichberg P, Spiegel A, Peled A, Brodie C, Seger R, Nagler A, Alon R and Lapidot T (2005) Atypical PKC-zeta regulates SDF-1-mediated migration and development of human CD34+ progenitor cells. *J Clin Invest* **115**:168-176.

Rajagopal S, Kim J, Ahn S, Craig S, Lam CM, Gerard NP, Gerard C and Lefkowitz RJ (2010) Beta-arrestin- but not G protein-mediated signaling by the "decoy" receptor CXCR7. *Proc Natl Acad Sci U S A* **107**:628-632.

Rangel-Moreno J, To JY, Owen T, Goldman BI, Smrcka AV and Anolik JH (2016) Inhibition of G protein betagamma subunit signaling abrogates nephritis in lupus prone mice. *Arthritis Rheumatol*.

Regner KR, Nozu K, Lanier SM, Blumer JB, Avner ED, Sweeney WE, Jr. and Park F (2011) Loss of activator of G-protein signaling 3 impairs renal tubular regeneration following acute kidney injury in rodents. *FASEB J* **25**:1844-1855.

Robichaux WG, 3rd, Oner SS, Lanier SM and Blumer JB (2015) Direct Coupling of a Seven-Transmembrane-Span Receptor to a Galphai G-Protein Regulatory Motif Complex. *Mol Pharmacol* **88**:231-237.

Rudolph U, Finegold MJ, Rich SS, Harriman GR, Srinivasan Y, Brabet P, Boulay G, Bradley A and Birnbaumer L (1995) Ulcerative colitis and adenocarcinoma of the colon in G alpha i2-deficient mice. *Nat Genet* **10**:143-150.

Sagar D, Lamontagne A, Foss CA, Khan ZK, Pomper MG and Jain P (2012) Dendritic cell CNS recruitment correlates with disease severity in EAE via CCL2 chemotaxis at the blood-brain barrier through paracellular transmigration and ERK activation. *J Neuroinflammation* **9**:245.

Schmidt N, Art J, Forsch I, Werner A, Erkel G, Jung M, Horke S, Kleinert H and Pautz A (2012) The anti-inflammatory fungal compound (S)-curvularin reduces proinflammatory gene expression in an in vivo model of rheumatoid arthritis. *J Pharmacol Exp Ther* **343**:106-114.

Downloaded from jpet.aspetjournals.org at ASPET Journals on April 24, 2024

JPET Fast Forward. Published on January 6, 2017 as DOI: 10.1124/jpet.116.238436
This article has not been copyedited and formatted. The final version may differ from this version.

Singh V, Raghuwanshi SK, Smith N, Rivers EJ and Richardson RM (2014) G Protein-coupled receptor kinase-6 interacts with activator of G protein signaling-3 to regulate CXCR2-mediated cellular functions. *J Immunol* **192**:2186-2194.

Skokowa J, Ali SR, Felda O, Kumar V, Konrad S, Shushakova N, Schmidt RE, Piekorz RP, Nurnberg B, Spicher K, Birnbaumer L, Zwirner J, Claassens JW, Verbeek JS, van Rooijen N, Kohl J and Gessner JE (2005) Macrophages induce the inflammatory response in the pulmonary Arthus reaction through G alpha i2 activation that controls C5aR and Fc receptor cooperation. *J Immunol* **174**:3041-3050.

Surve CR, Lehmann D and Smrcka AV (2014) A chemical biology approach demonstrates G protein betagamma subunits are sufficient to mediate directional neutrophil chemotaxis. *J Biol Chem* **289**:17791-17801.

Surve CR, To JY, Malik S, Kim M and Smrcka AV (2016) Dynamic regulation of neutrophil polarity and migration by the heterotrimeric G protein subunits Galphai-GTP and Gbetagamma. *Sci Signal* **9**:ra22.

Takesono A, Cismowski MJ, Ribas C, Bernard M, Chung P, Hazard S, 3rd, Duzic E and Lanier SM (1999) Receptor-independent activators of heterotrimeric G-protein signaling pathways. *J Biol Chem* **274**:33202-33205.

Tilton B, Ho L, Oberlin E, Loetscher P, Baleux F, Clark-Lewis I and Thelen M (2000) Signal transduction by CXC chemokine receptor 4. Stromal cell-derived factor 1 stimulates prolonged protein kinase B and extracellular signal-regulated kinase 2 activation in T lymphocytes. *J Exp Med* **192**:313-324.

Vural A, Al-Khodor S, Cheung GY, Shi CS, Srinivasan L, McQuiston TJ, Hwang IY, Yeh AJ, Blumer JB, Briken V, Williamson PR, Otto M, Fraser ID and Kehrl JH (2015) Activator of G-Protein Signaling 3-Induced Lysosomal Biogenesis Limits Macrophage Intracellular Bacterial Infection. *J Immunol* **196**:846-856.

Downloaded from jpet.aspetjournals.org at ASPET Journals on April 24, 2024

JPET Fast Forward. Published on January 6, 2017 as DOI: 10.1124/jpet.116.238436
This article has not been copyedited and formatted. The final version may differ from this version.

Warnock RA, Askari S, Butcher EC and von Andrian UH (1998) Molecular mechanisms of lymphocyte homing to peripheral lymph nodes. *J Exp Med* **187**:205-216.

Wiege K, Ali SR, Gewecke B, Novakovic A, Konrad FM, Pexa K, Beer-Hammer S, Reutershan J, Piekorz RP, Schmidt RE, Nurnberg B and Gessner JE (2013) Galphai2 is the essential Galphai protein in immune complex-induced lung disease. *J Immunol* **190**:324-333.

Wiege K, Le DD, Syed SN, Ali SR, Novakovic A, Beer-Hammer S, Piekorz RP, Schmidt RE, Nurnberg B and Gessner JE (2012) Defective macrophage migration in Galphai2- but not Galphai3-deficient mice. *J Immunol* **189**:980-987.

Yan C, Ding X, Dasgupta N, Wu L and Du H (2012) Gene profile of myeloid-derived suppressive cells from the bone marrow of lysosomal acid lipase knock-out mice. *PLoS One* **7**:e30701.

Yao L, McFarland K, Fan P, Jiang Z, Inoue Y and Diamond I (2005) Activator of G protein signaling 3 regulates opiate activation of protein kinase A signaling and relapse of heroin-seeking behavior. *Proc Natl Acad Sci U S A* **102**:8746-8751.

Yao L, McFarland K, Fan P, Jiang Z, Ueda T and Diamond I (2006) Adenosine A2a blockade prevents synergy between mu-opiate and cannabinoid CB1 receptors and eliminates heroin-seeking behavior in addicted rats. *Proc Natl Acad Sci U S A* **103**:7877-7882.

Zabel BA, Wang Y, Lewen S, Berahovich RD, Penfold ME, Zhang P, Powers J, Summers BC, Miao Z, Zhao B, Jalili A, Janowska-Wieczorek A, Jaen JC and Schall TJ (2009) Elucidation of CXCR7-mediated signaling events and inhibition of CXCR4-mediated tumor cell transendothelial migration by CXCR7 ligands. *J Immunol* **183**:3204-3211.

Zarbock A, Deem TL, Burcin TL and Ley K (2007) Galphai2 is required for chemokine-induced neutrophil arrest. *Blood* **110**:3773-3779.

Zhang Y, Tang W, Jones MC, Xu W, Halene S and Wu D (2010) Different roles of G protein subunits beta1 and beta2 in neutrophil function revealed by gene expression silencing in primary mouse neutrophils. *J Biol Chem* **285**:24805-24814.

Downloaded from jpet.aspetjournals.org at ASPET Journals on April 24, 2024

JPET Fast Forward. Published on January 6, 2017 as DOI: 10.1124/jpet.116.238436
This article has not been copyedited and formatted. The final version may differ from this version.

Zhao P, Nguyen CH and Chidiac P (2010) The proline-rich N-terminal domain of G18 exhibits a novel G protein regulatory function. *J Biol Chem* **285**:9008-9017.

Zhong J, Kim MS, Chaerkady R, Wu X, Huang TC, Getnet D, Mitchell CJ, Palapetta SM, Sharma J, O'Meally RN, Cole RN, Yoda A, Moritz A, Loriaux MM, Rush J, Weinstock DM, Tyner JW and Pandey A (2012) TSLP signaling network revealed by SILAC-based phosphoproteomics. *Mol Cell Proteomics* **11**:M112 017764.

Downloaded from jpet.aspetjournals.org at ASPET Journals on April 24, 2024

JPET Fast Forward. Published on January 6, 2017 as DOI: 10.1124/jpet.116.238436
This article has not been copyedited and formatted. The final version may differ from this version.

FOOTNOTES

This work was supported by National Institutes of Health (NIH) National Institute of General Medical Sciences [grant R01-GM086510 to J.B.B.], National Institute of General Medical Sciences South Carolina Institutional Development Awards (IDeA) Networks of Biomedical Research Excellence (SC-INBRE) [grant P20-GM103499 to M.B.O.], National Cancer Institute [grant T32-CA119945 to M.B.O.), , MUSC institutional funds (to J.B.B.) and the intramural research program of the National Institute of Allergy and Infectious Diseases (to J.H.K.). This work was also enabled by support from the National Institutes of Health National Institute on Neurological Diseases and Stroke [grant R01-NS24821] and National Institute on Drug Abuse [grant R01-DA025896], both to Dr. Stephen M. Lanier (Wayne State University). The research presented in this article was supported in part by the Flow Cytometry and Cell Sorting Shared Resource, funded by a Cancer Center Support grant from the National Cancer Institute [P30 CA138313 to the Hollings Cancer Center at the Medical University of South Carolina] and in part by the National Center for Research Resources and the Office of the Director of the National Institutes of Health [grant number C06 RR015455 to the Hollings Cancer Center at the Medical University of South Carolina].

Present Address (W.G.R): University of Texas Health Science Center – Houston, Houston, TX

Present Address (A.V.): Department of Pharmacology, Wayne State University, Detroit, MI (AV)

[1] Cho, H., Kehrl, J.H. and Blumer, J.B. Unpublished observations.

[2] Robichaux, W. G. III, Branham-O'Connor, M. and Blumer, J.B. Unpublished observations.

[3] Hwang, I-Y., Vural, A. and Kehrl, J.H. Unpublished observations.

Downloaded from jpet.aspetjournals.org at ASPET Journals on April 24, 2024

JPET Fast Forward. Published on January 6, 2017 as DOI: 10.1124/jpet.116.238436
This article has not been copyedited and formatted. The final version may differ from this version.

FIGURE LEGENDS

Figure 1. Regulation of Gαi$_2$-AGS4 interaction by the prototype chemokine receptor CXCR4. (A) Top panel – Schematic of bioluminescence resonance energy transfer (BRET) system along with representation of hypothesized agonist-induced regulation of Gαi$_2$YFP – AGS4-Rluc BRET association by receptor activation. For simplification, AGS4-Rluc is shown interacting with a single Gαi$_2$-YFP; however, AGS4 can bind multiple Gαi subunits simultaneously (Kimple et al., 2004; Oner et al., 2010b)[2], which may be responsible for the robust BRET signals observed (Oner et al., 2010b). Bottom panel – Net BRET signals were obtained from HEK 293 cells transfected with 2 ng phRLuc$_{N3}$::AGS4 or 2 ng phRLuc$_{N3}$::AGS4-Q/A-Rluc and 500 ng pcDNA3::Gαi$_2$-YFP. Cells were also transfected in the presence or absence of 500 ng pcDNA3::CXCR4. Vehicle (Tyrode's solution) or CXCL12 (100 ng/mL) were added to cells as indicated followed by fluorescence and luminescence readings as described in "Materials and Methods." The CXCR4 antagonist AMD3100 (plerixafor, 1 μg/mL) was added 10 minutes prior to agonist stimulation as indicated. Cells were treated with pertussis toxin (PTX, 100 ng/mL) 18 hours prior to receptor stimulation where indicated. Data are expressed as means ± SEM from 3 independent experiments with triplicate determinations (n = 9). *, p-value < 0.0001 as compared with vehicle treated control group as determined by one-way ANOVA with Tukey's post-hoc test. (B) Top panel – Schematic representing the BRET system used to measure effect of chemokine receptor activation on the proximity of Gαi-AGS4 complex to CXCR4-Venus. Bottom panel – HEK cells were transfected with 2 ng phRLucN3::AGS4 or 2 ng phRLucN3::AGS4-Q/A along with 750 ng pIRESpuro3::CXCR4-Venus in the presence or absence of 750 ng pcDNA3::Gαi2 as indicated. Vehicle (Tyrode's solution) or CXCL12 (100 ng/mL) were added to cells as indicated followed by fluorescence and luminescence readings as described in "Experimental Procedures." The CXCR4 antagonist AMD3100 (plerixafor, 1 μg/mL) was added 10 minutes prior to agonist stimulation as indicated. Cells were treated with pertussis toxin (PTX, 100

Downloaded from jpet.aspetjournals.org at ASPET Journals on April 24, 2024

JPET Fast Forward. Published on January 6, 2017 as DOI: 10.1124/jpet.116.238436
This article has not been copyedited and formatted. The final version may differ from this version.

ng/mL) 18 hours prior to receptor stimulation where indicated. Data are expressed as means ± SEM from at least 3 independent experiments with triplicate determinations (n = 9). *, p-value < 0.0001 as compared with vehicle treated control group as determined by one-way ANOVA with Tukey's post-hoc test.

Figure 2. Loss of AGS4 results in altered leukocyte population phenotype. (A) Left panel – A three-primer PCR approach was used to genotype AGS4/Gpsm3 wild-type ($^{+/+}$), heterozygous ($^{+/-}$) and null ($^{-/-}$) mice. Right panel – schematic depicting the strategy used to generate and PCR genotype AGS4/Gpsm3-null mice as described in Materials and Methods. DNA primers *a*, *b* and *c* (corresponding to "Gpsm3 16651 forward," "Common 3' forward" and "CSD-Gpsm3-SR1," respectively; see Materials and Methods for additional details) were used in a three-primer PCR reaction in which a wild-type product at 1200 bp resulted from priming from primers *a* and *b*, and an AGS4/Gpsm3$^{-/-}$ product at 776 bp resulted from priming from primers *b* and *c*. (B) Lysates (100 μg per lane) from primary immature dendritic cells (iDC), mature dendritic cells (mDC) (left panel) and splenocytes (right panel) from WT and Gpsm3-null mice were subjected to SDS-PAGE, transferred to PVDF membranes and immunoblotted with AGS4 antisera as described in Experimental Procedures. "+C" refers to lysate prepared from HEK293 cells transfected with pcDNA3::AGS4 after 24h as described in Experimental Procedures. (C) Complete blood count (CBC) analysis from blood collected from WT and AGS4/Gpsm3-null mice as described in Experimental Procedures. Percent of leukocyte populations in relation to total number of white blood cells was calculated and compared between WT and AGS4/Gpsm3-null littermate pairs. Data are represented as the mean +/- S.E. from 4 pairs of 12-week old mice.

Figure 3. AGS4-KO dendritic cells and splenocytes exhibit defects in CXCL12-stimulated phosphorylation of ERK1/2. Single cell suspensions of WT and AGS4/Gpsm3-null cultured dendritic cells (A) or splenocytes (B) were treated with 200 ng/mL CXCL12 as described in Experimental Procedures. At the indicated times, cells were lysed in 1% NP40 lysis buffer containing protease and phosphatase inhibitors, subjected to SDS-PAGE (50 μg per lane), transferred to PVDF and

Downloaded from jpet.aspetjournals.org at ASPET Journals on April 24, 2024

JPET Fast Forward. Published on January 6, 2017 as DOI: 10.1124/jpet.116.238436
This article has not been copyedited and formatted. The final version may differ from this version.

immunoblotted with anti-phospho-Erk (Y204) and total Erk-specific antibodies. Representative immunoblots are shown in the upper panels and densitometric analysis of at least 3 independent experiments (represented as means ± S.E.) are shown in the lower panels (* denotes $p < 0.05$).

Figure 4. Loss of AGS4 results in defective chemotaxis in primary leukocytes. (A) Bone marrow-derived dendritic cells (BMDCs) from WT and AGS4/Gpsm3-null mice were prepared as described in Experimental Procedures. BMDCs were loaded in transwell migration chambers with the bottom chamber containing serum-free RPMI in the absence and presence of 10, 50, 100, 250, 500 ng/mL CXCL12 as indicated. After 20h at 37°C, cells in the bottom chamber were counted, and the percentage of cells migrated was calculated relative to the input where the number of cells migrating to vehicle only was subtracted. Data are represented as the mean +/- S.E. of at minimum 4 independent experiments with at least triplicate determinations (* denotes $p < 0.01$). (B) T lymphocytes were isolated from freshly harvested splenocytes of WT and AGS4/Gpsm3-null mice following red blood cell lysis and filtering to remove cell and tissue aggregates as described in Experimental Procedures. Cells were loaded in transwell migration chambers with bottom chambers containing serum-free RPMI in the absence or presence of 50, 150, 300 ng/mL CCL19. After 5h at 37°C, cells in the bottom chamber were counted, and the percentage of cells migrated was calculated relative to the input where the number of cells migrating to vehicle only was subtracted. Data are represented as the mean +/- S.E. of at minimum 4 independent experiments with at least triplicate determinations (* denotes $p < 0.01$).

Figure 5. AGS4-KO neutrophils demonstrate reduced migration to site of inflammation. (A,B) Neutrophils were isolated from freshly harvested bone marrow from WT and AGS4/Gpsm3-null mice using Percoll gradient centrifugation as described in Experimental Procedures. (A) Neutrophil lysates (100 μg) were prepared with 1% NP-40 lysis buffer and subjected to SDS-PAGE, transferred to PVDF and immunoblotted with AGS4 antisera as described in Experimental Procedures. The representative immunoblot shown is reflective of at least 3 independent experiments. (B) Isolated neutrophils were

Downloaded from jpet.aspetjournals.org at ASPET Journals on April 24, 2024

JPET Fast Forward. Published on January 6, 2017 as DOI: 10.1124/jpet.116.238436
This article has not been copyedited and formatted. The final version may differ from this version.

loaded in transwell migration chambers with the bottom chamber containing serum-free RPMI in the absence and presence of 0.1, 1.0, 5.0 μM fMLP. After 3h at 37°C, cells in the bottom chamber were counted, and the percentage of cells migrated was calculated relative to the input where the number of cells migrating to vehicle only was subtracted. (C) WT and AGS4/Gpsm3-null mice received 1 mL intraperitoneal injections of 4% thioglycollate or sterile phosphate buffered saline (PBS) to induce localized inflammation as described in Experimental Procedures. Two hours post-injection, mice were euthanized and the intraperitoneal cavity was lavaged with 10 ml cold, sterile PBS (left panel). Blood (middle panel) was collected by cardiac stick and femurs were processed to harvest bone marrow cells (right panel) as described in Experimental Procedures. Red blood cells were lysed from cell preps and remaining cells were stained with CD11b–FITC and Ly6G–PE for flow cytometry analysis of neutrophil numbers in each tissue. Neutrophil cell numbers were calculated using total events collected, applying flow rate and percentage of dual positive cells followed by dilutions carried out during processing of the cells. Data are represented as the mean +/- S.E. of n = 4 mice per genotype. *, $p < 0.05$.

Downloaded from jpet.aspetjournals.org at ASPET Journals on April 24, 2024

Figure 1

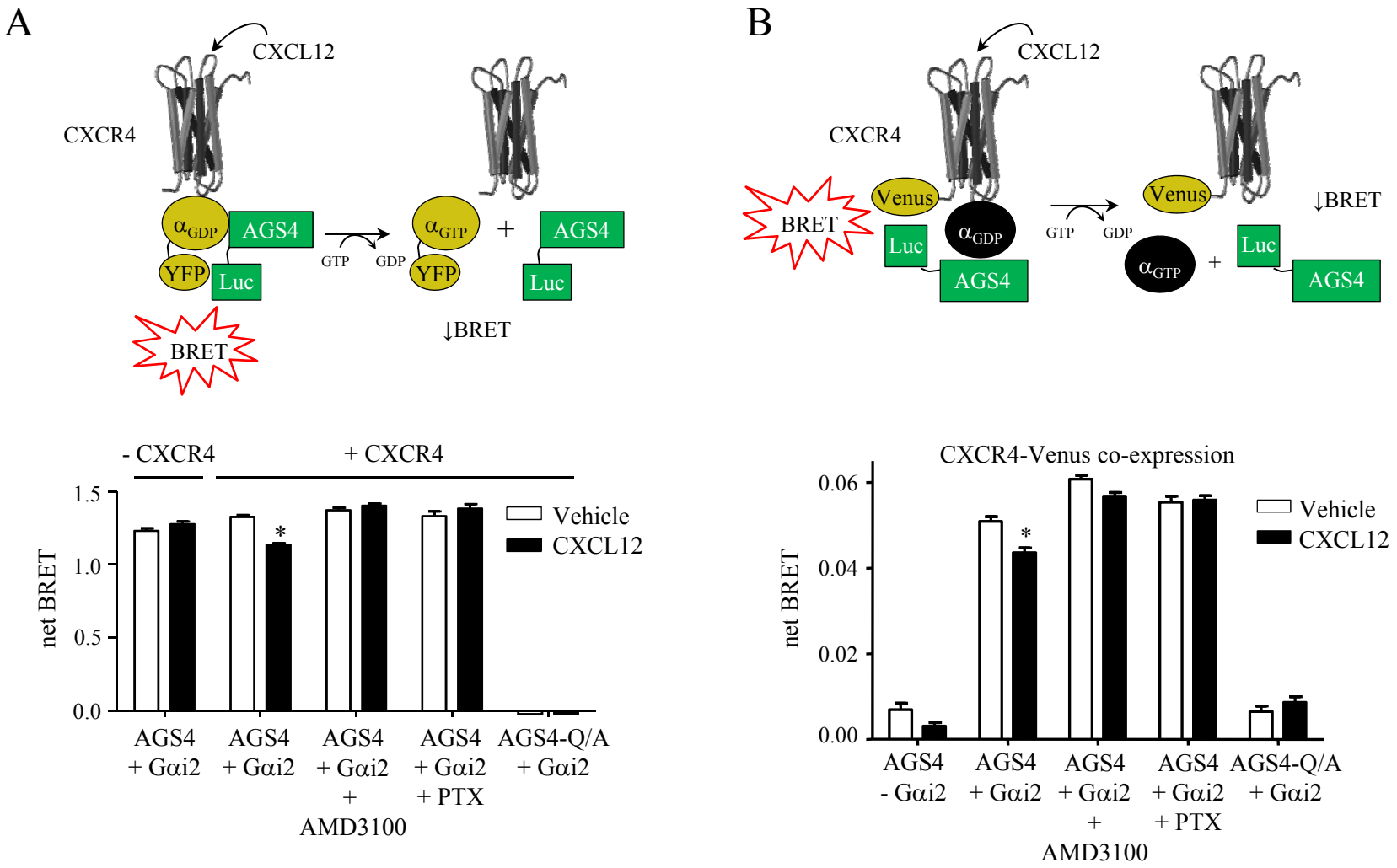

JPET Fast Forward. Published on January 6, 2017 as DOI: 10.1124/jpet.116.238436
This article has not been copyedited and formatted. The final version may differ from this version.

Downloaded from jpet.aspetjournals.org at ASPET Journals on April 24, 2024

Figure 2

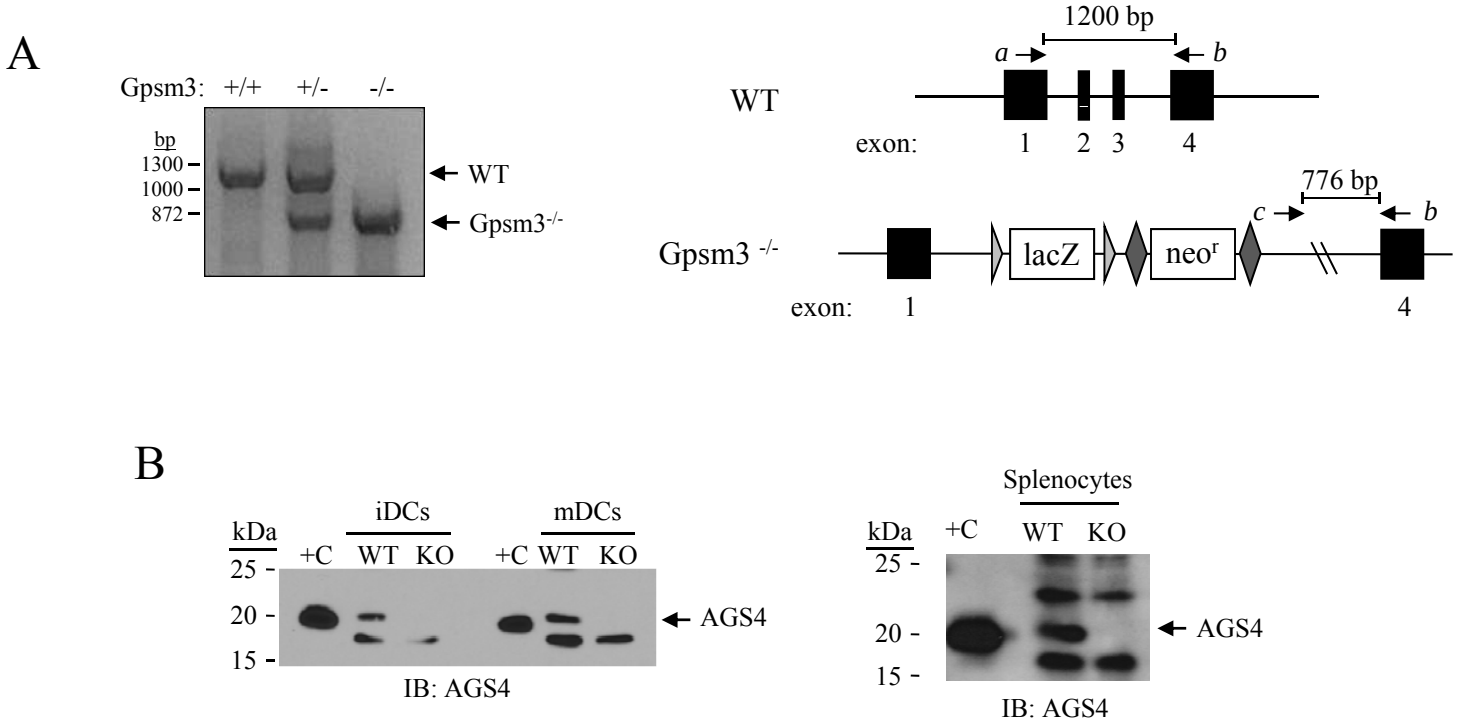

JPET Fast Forward. Published on January 6, 2017 as DOI: 10.1124/jpet.116.238436
This article has not been copyedited and formatted. The final version may differ from this version.

Downloaded from jpet.aspetjournals.org at ASPET Journals on April 24, 2024

Figure 3

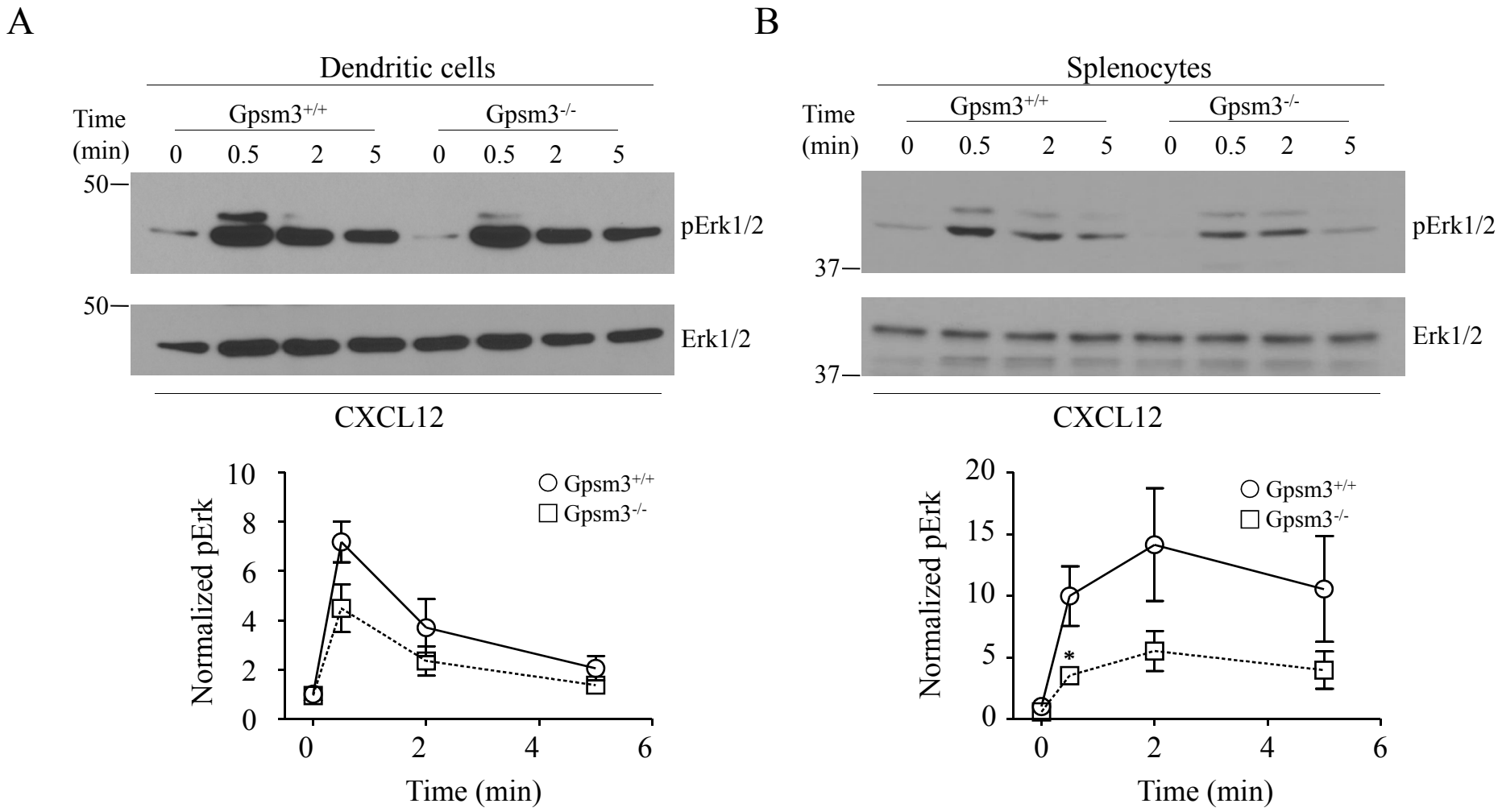

JPET Fast Forward. Published on January 6, 2017 as DOI: 10.1124/jpet.116.238436
This article has not been copyedited and formatted. The final version may differ from this version.

Downloaded from jpet.aspetjournals.org at ASPET Journals on April 24, 2024

Figure 4

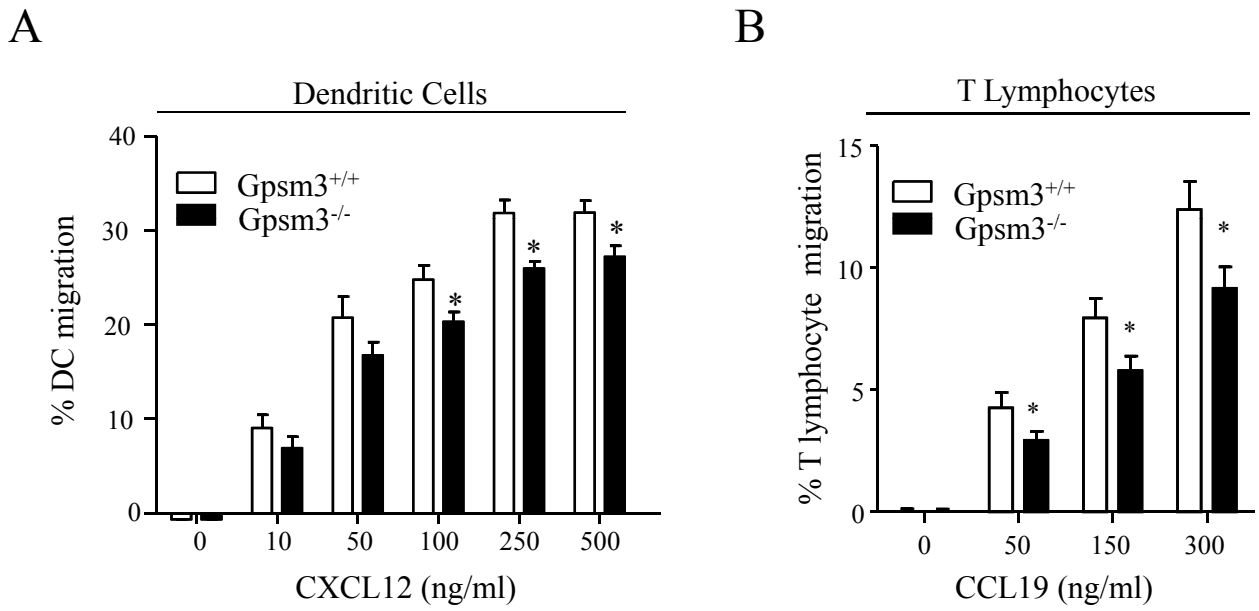

JPET Fast Forward. Published on January 6, 2017 as DOI: 10.1124/jpet.116.238436
This article has not been copyedited and formatted. The final version may differ from this version.

Downloaded from jpet.aspetjournals.org at ASPET Journals on April 24, 2024

Figure 5

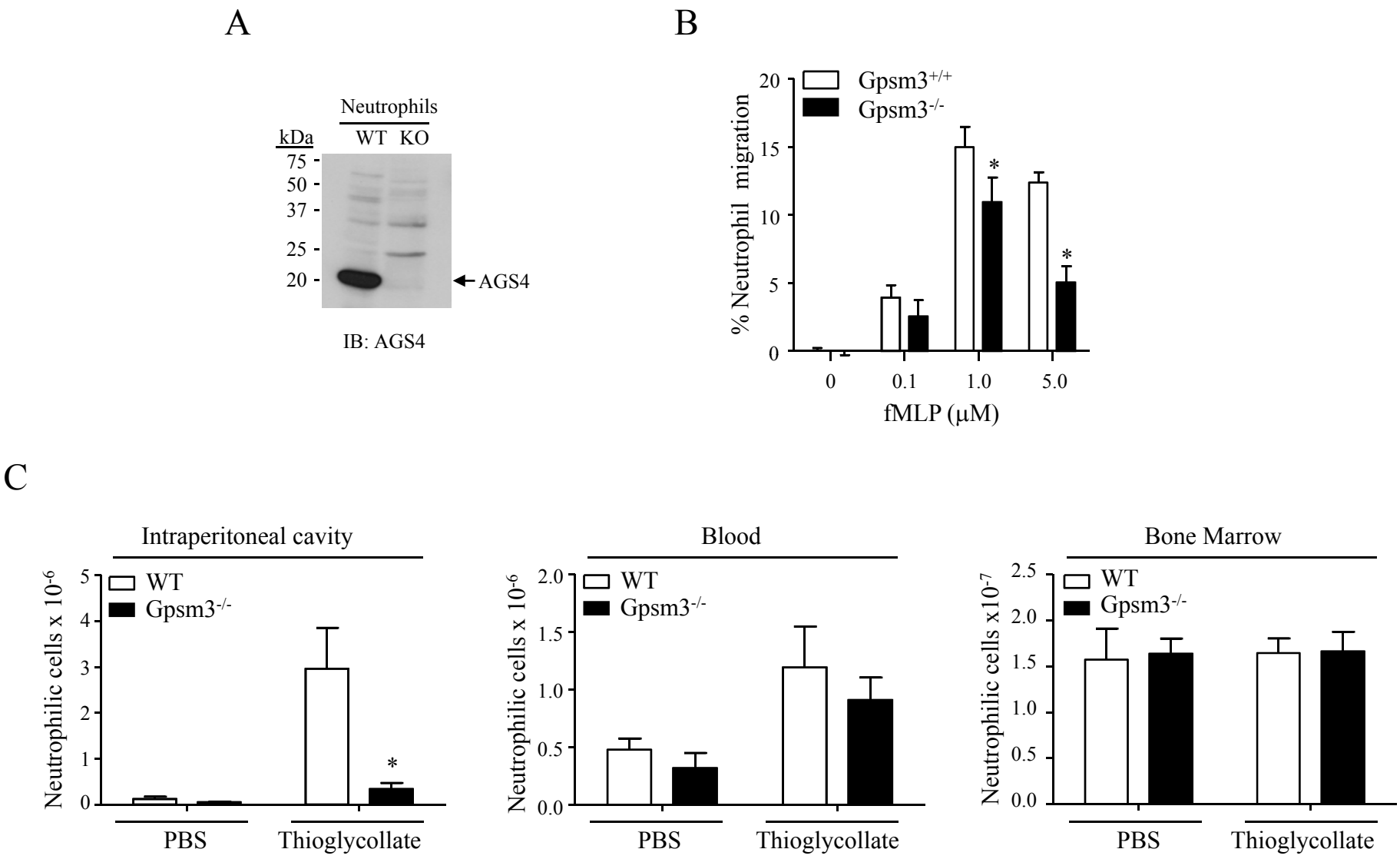

JPET Fast Forward. Published on January 6, 2017 as DOI: 10.1124/jpet.116.238436
This article has not been copyedited and formatted. The final version may differ from this version.

Downloaded from jpet.aspetjournals.org at ASPET Journals on April 24, 2024